Redox Biology 10 (2016) 65–77

Contents lists available at ScienceDirect

Redox Biology

journal homepage: www.elsevier.com/locate/redox

Blood cell respirometry is associated with skeletal and cardiac muscle bioenergetics: Implications for a minimally invasive biomarker of mitochondrial health

Daniel J. Tyrrell [a], Manish S. Bharadwaj [a], Matthew J. Jorgensen [b], Thomas C. Register [b], Anthony J.A. Molina [a,*]

[a] Sticht Center on Aging & Department of Internal Medicine, Section on Gerontology and Geriatrics, Wake Forest School of Medicine, Winston-Salem, NC 27157, USA
[b] Department of Pathology, Section on Comparative Medicine, Wake Forest School of Medicine, Winston-Salem, NC 27157, USA

ARTICLE INFO

Article history:
Received 16 September 2016
Accepted 20 September 2016
Available online 21 September 2016

Keywords:
Mitochondria
Bioenergetics
Blood cells
Muscle
Cellular respiration

ABSTRACT

Blood based bioenergetic profiling strategies are emerging as potential reporters of systemic mitochondrial function; however, the extent to which these measures reflect the bioenergetic capacity of other tissues is not known. The premise of this work is that highly metabolically active tissues, such as skeletal and cardiac muscle, are susceptible to differences in systemic bioenergetic capacity. Therefore, we tested whether the respiratory capacity of blood cells, monocytes and platelets, are related to contemporaneous respirometric assessments of skeletal and cardiac muscle mitochondria. 18 female vervet/African green monkeys (*Chlorocebus aethiops sabaeus*) of varying age and metabolic status were examined for this study. Monocyte and platelet maximal capacity correlated with maximal oxidative phosphorylation capacity of permeabilized skeletal muscle (R=0.75, 95% confidence interval [CI]: 0.38–0.97; R=0.51, 95%CI: 0.05–0.81; respectively), isolated skeletal muscle mitochondrial respiratory control ratio (RCR; R=0.70, 95%CI: 0.35–0.89; R=0.64, 95%CI: 0.23–0.98; respectively), and isolated cardiac muscle mitochondrial RCR (R=0.55, 95%CI: 0.22–0.86; R=0.58, 95%CI: 0.22–0.85; respectively). These results suggest that blood based bioenergetic profiling may be used to report on the bioenergetic capacity of muscle tissues. Blood cell respirometry represents an attractive alternative to tissue based assessments of mitochondrial function in human studies based on ease of access and the minimal participant burden required by these measures.

1. Introduction

Mitochondrial dysfunction is well recognized to play a key role in a wide variety of diseases, particularly those associated with aging. For this reason, assessments of mitochondrial function have long been proposed to have significant diagnostic and prognostic applications. There is mounting evidence that blood cells can report on systemic mitochondrial function. Diabetes, atherosclerosis, and neurodegeneration are all related to the deterioration of various mitochondrial parameters in multiple cell types, including leukocytes and platelets [1–4]. Changes in mitochondrial DNA (mtDNA), mitochondrial enzyme activity, and electron transport chain (ETC) activity measured in peripheral blood mononuclear cells, monocytes, lymphocytes, and platelets have been associated with mortality, diabetes, HIV, cardiovascular disease, Parkinson's disease, Alzheimer's disease, cancer, inflammation, cognition, Huntington's disease, sepsis, and fibromyalgia [1,5–18]. More recently, blood based bioenergetic profiling strategies utilizing cellular respirometry have been associated with key features of aging such as gait speed, physical function decline, inflammation, and depression [19–21].

Blood based measures of mitochondrial function may provide a minimally invasive test that is particularly well suited for diagnostic use. In addition, these measures are highly amenable for use in large scale clinical trials, including those with serial longitudinal assessments, because they require minimal patient burden and

Abbreviations: ACD, acid citrate dextrose; BMI, body mass index; BSA, bovine serum albumin; CP, Chappell-Perry buffer; CII, complex 2; EGTA, triethylene glycol diammine tetraacetic acid; ELISA, enzyme-linked immunosorbent assay; ETC, electron transport chain; FCCP, Carbonyl cyanide-4-(trifluoromethoxy)phenylhydrazone; HOMA-IR, homeostatic model assessment of insulin resistance; MAS, mannitol and sucrose buffer; MAX, maximal FCCP-linked bioenergetic capacity; MES, 2-(N-morpholino)ethanesulfonic acid; O2k, Oroboros Oxygraph 2K; OXPHOS, oxidative phosphorylation; PBS, phosphate buffered saline; PGE_1, prostaglandin E_1; PmFBs, permeabilized fiber bundles; RCR, respiratory control ratio; SD, standard deviation; XF, extracellular flux

* Corresponding author.
E-mail address: amolina@wakehealth.edu (A.J.A. Molina).

http://dx.doi.org/10.1016/j.redox.2016.09.009

cost compared to biopsy based measures of mitochondrial function. Blood based bioenergetic profiling strategies are also well suited for use in older adults who often present with multiple contraindications to biopsy. However, little is known about whether these blood based measurements are able to recapitulate measures of mitochondrial function performed in other tissues.

In this study, we examined the relationships of monocyte and platelet mitochondrial respiration with assessments of mitochondrial function performed in muscle tissues. We focused on skeletal and cardiac muscle because age-related bioenergetic decline is thought to be most significant in highly metabolically active tissues and based on our previous findings that blood based respirometry is positively correlated with measures of physical function and strength in human subjects [20]. For example, skeletal muscle from older adults is reported to have reduced ATP production, maximal bioenergetic capacity, and mitochondrial content compared to younger counterparts [22]. In addition, cardiac tissue oxidative capacity and phosphocreatine/ATP ratio are reduced in the earliest stages of heart failure in humans [23], which is further impaired by diabetes and obesity [24,25]. These are similar to findings from rodent models [26,27]. The use of a non-human primate model provided us with reliable access to heart and skeletal muscle tissue and sufficient volumes of blood to permit the analyses of multiple blood cell populations. Vervet macaques are susceptible to naturally occurring changes in body composition [28], physical function [29], and chronic diseases ranging from obesity [30], diabetes [31], and heart disease [32] as they age in a manner similar to humans [33]. The present study utilized a group of female vervet macaques specifically selected to represent a wide range of metabolic health status and insulin resistance as well as body mass indices from lean to obese across young and old age groups. This design was utilized in order to maximize the potential bioenergetic differences between animals.

Blood cell respiration was compared to skeletal muscle mitochondrial function in two ways. *Vastus lateralis* muscle fibers were permeabilized and analyzed by high resolution respirometry [34] to examine bioenergetic capacity in a manner that maintains potential differences in mitochondrial content and architecture [35]. In addition, we examined respiratory control in isolated *vastus lateralis* mitochondria [36] to determine whether blood based measures might be related to differences in intrinsic electron transport chain function. Similar methods using isolated organelles were carried out for analysis of cardiac muscle mitochondrial function. We hypothesized that because blood cells are continuously exposed to circulating factors such as inflammatory cytokines, redox stress [37], and recently described mitokines [38]; which are known to affect mitochondrial function across tissues; respirometric analyses of monocytes and platelets will recapitulate differences in systemic bioenergetic capacity.

2. Materials and methods

2.1. Animal participants

This study included 18 female vervet/African green monkeys (*Chlorocebus aethiops sabaeus*) ranging in age from 8.2 to 23.4 yrs. The monkeys originally lived in stable social groups of 11–49 in indoor-outdoor housing units with approximately 28 m^2 indoors and 111 m^2 outdoors which contained perches, platforms, elevated climbing structures and a base composed of smooth stones. Seven of the 18 animals were moved to indoor housing (pair- or individually-housed) prior to study initiation. All animals were fed a standard monkey chow diet (LabDiet 1538), supplemented with fruits and vegetables 5 times per week. Water was available ad libitum. Blood samples were obtained from anesthetized animals immediately prior to necropsy, and the harvest of skeletal and cardiac muscle tissues. Euthanasia was carried out with IM ketamine (10–15 mg/kg) followed by IV sodium pentobarbital (60–100 mg/kg) to attain deep surgical anesthesia and exsanguination in accordance with guidelines established by the Panel on Euthanasia of the American Veterinary Medical Association. All procedures were approved and performed according to the guidelines of state and federal laws, the US Department of Health and Human Services, and the Animal Care and Use Committee of Wake Forest School of Medicine.

2.2. Body mass measurements

BMI was estimated as the ratio of body mass to the square of trunk length measured from the suprasternal notch to the pubic symphysis using an electronic caliper (in kg/m^2) and was calculated 4 months prior to necropsy while weight was measured at the time of necropsy [39].

2.3. Insulin, glucose, and insulin sensitivity measurements

Fasting glucose was determined using reagents and instrumentation (ACE ALERA autoanalyzer) from Alfa Wasserman Diagnostic Technologies (West Caldwell, NJ). Insulin was determined by an enzyme-linked immunosorbent assay (ELISA; Mercodia, Uppsala, Sweden). All analyses were performed in the Wake Forest Comparative Medicine Clinical Chemistry and Endocrinology Laboratory 4 months prior to necropsy. Homeostatic model of insulin resistance (HOMA-IR)=([mg/dL fasting glucose X mIU/L fasting insulin]/405) was used as an estimate of insulin resistance [40].

2.4. Isolation of blood cells

Blood (8 mL) was collected from fasted monkeys into acid citrate dextrose (ACD) tubes (Vacutainer; Becton Dickinson, Franklin Lakes, NJ) and processed immediately to obtain platelet and CD14+ monocyte preparations. Platelets and CD14+ monocytes were isolated using methods similar to those described by Chacko et al. [41]. Briefly, whole blood in ACD tubes was centrifuged at $500 \times g$ for 15 min at room temperature with the brake off. Platelet rich plasma was removed and platelets were isolated by centrifugation at $1500 \times g$ for 10 min, washed in phosphate-buffered saline (PBS) with prostaglandin E_1 (PGE1; Cayman Chemical, Ann Arbor, MI), and resuspended in extracellular flux (XF) assay buffer (Seahorse Biosciences, North Billerica, MA) containing 1 mM Na^+-pyruvate, 1 mM GlutaMAX (Gibco, Grand Island, NY), 11 mM D-glucose, and PGE1 (pH 7.4) for respirometry experiments. The buffy coat layer was extracted, diluted 4× in RPMI 1640 (Gibco) and layered onto 3 mL of polysucrose solution at a density of 1.077 g/mL (Sigma Histopaque®-1077, St. Louis, MO) in 15 mL centrifuge tubes and centrifuged at $700 \times g$ for 30 min with no brake. The buffy coat layer was obtained, washed in PBS, and divided into 2 tubes. CD14+ monocytes were isolated from 1 tube using CD14-labeled magnetic microbeads (Miltenyi Biotec, San Diego, CA) according to manufacturer instructions using modified RPMI 1640+fatty-acid free bovine serum albumin (BSA) media. Monocytes were washed in modified RPMI 1640 media and resuspended in XF assay buffer without PGE1 for respirometry experiments.

2.5. Respirometry of blood cells

A total of 250,000 monocytes and 25,000,000 platelets per well were plated in quadruplicate in the Seahorse microplate. Bioenergetic profiling using selected inhibitors and uncoupler have

previously been described [42]. Briefly, basal oxygen consumption rate (OCR) measures were monitored while the cells respired in XF assay buffer, followed by sequential additions of oligomycin (750 nM), carbonyl cyanide-4-(trifluoromethoxy) phenylhydrazone (FCCP; 1 μM), and antimycin-A+rotenone (A/R; both 1 μM) (all from Sigma) with measurements taken after each addition. MAX OCR was calculated after addition of FCCP, a potent mitochondrial uncoupler. The use of FCCP as a chemical uncoupler allows us to estimate maximal ETC activity and the supply of substrates available for respiration. Reserve capacity was calculated as the difference between MAX and the basal OCR [43,44]. The difference between the measurement taken after the oligomycin addition (oligo) and the A/R addition is reported as the leak respiration and the difference between basal and oligo is the OCR attributed to ATP [45]. Platelet respiration was normalized to mg protein, determined by Pierce BCA assay (ThermoFisher Scientific, Grand Island, NY).

2.6. Preparation of permeabilized skeletal muscle fiber bundles

Approximately 1 g of skeletal muscle tissue was obtained immediately after euthanasia. A portion of each muscle sample was immediately placed in ice-cold buffer X (50 mM K-MES, 7.23 mM K_2EGTA, 2.77 mM CaK_2EGTA, 20 mM imidazole, 20 mM taurine, 5.7 mM ATP, 14.3 mM phosphocreatine and 6.56 mM $MgCl_2 \cdot 6H_2O$, pH 7.1) for preparation of permeabilized muscle fiber bundles (PmFBs), as previously described [46]. About 2–4 mg fiber bundles were separated along the longitudinal axis using needle-tipped forceps under magnification, permeabilized with saponin (30 μg mL^{-1}) for 30 min at 4 °C, and subsequently washed in ice-cold buffer Z (105 mM K-MES, 30 mM KCl, 1 mM EGTA, 10 mM K_2HPO_4, 5 mM $MgCl_2 \cdot 6H_2O$, 0.5 mg mL^{-1} BSA, pH 7.4) for ~15 min prior to analysis. At the conclusion of each experiment, PmFBs were washed in double-distilled H_2O to remove salts, dried under vacuum, and weighed. Typical fiber bundle sizes were 0.2–0.6 mg dry weight.

2.7. Respirometry of permeabilized skeletal muscle fiber bundles

High-resolution O_2 consumption measurements were conducted in 2 mL of buffer Z containing 20 mM creatine and 25 μM blebbistatin to inhibit contraction [46] using the OROBOROS Oxygraph-2k (O2k; Oroboros Instruments, Innsbruck, Austria) [34]. Polarographic O_2 measurements were acquired at 2-s intervals with the steady state rate of respiration calculated from a minimum of 40 data points and expressed as pmol s^{-1} per mg dry weight. All respiration measurements were conducted at 37 °C and a working range [O_2] of ~350–180 μM. Respiration was measured in duplicate as follows: 2 mM malate (leak), 5 mM ADP, 5 mM pyruvate, 10 mM glutamate (complex I OXPHOS substrates), followed by sequential additions of 10 mM succinate (complex II OXPHOS substrates), 1 μM cytochrome c to test for mitochondrial membrane integrity, and sequential titrations of 1 mM FCCP (MAX), and 2.5 μM antimycin-A +0.5 μM rotenone (non-mitochondrial respiration).

2.8. Isolation of mitochondria from skeletal and cardiac muscle

Mitochondria were isolated as previously described [36,47] from both skeletal and cardiac muscle. For each animal, ~50 mg of tissue was minced into small pieces and resuspended in Chappell-Perry Buffer I (CP I) containing ~1 mg/mL Nagarse. After incubation with Nagarse for 5 min at room temperature, homogenization was performed using a Bio Gen series Model PRO200 homogenizer (Pro-Scientific, Inc., Oxford, CT) equipped with a 5 mm PRO quick connect generator probe. The homogenized tissue was washed with an equal volume of CP I and 2X volume of CP II buffer by centrifuging at 600 × G at 4 °C for 10 min (Eppendorf centrifuge 5804R, Eppendorf AG, Hamburg, Germany). The resulting supernatant was filtered through cheese cloth and the filtrate centrifuged at 10,000 × *g* at 4 °C for 10 min using a Beckman centrifuge, model J2-21M Induction drive centrifuge (Beckman-Coulter, Inc., Brea, CA) to obtain a mitochondrial pellet. The pellet was further washed first with CP II and then with CP I buffer. Finally, the pellet was suspended in mitochondrial assay solution (mannitol and sucrose buffer: MAS; sucrose 35 mM, mannitol 110 mM, KH_2PO_4 2.5 mM, $MgCl_2$ 2.5 mM, HEPES 1.0 mM, EGTA 0.5 mM, fatty-acid free BSA 0.10%, pH 7.4) prior to respirometry. Purified mitochondrial protein was determined according to manufacturer's instructions by Pierce BCA assay (ThermoFisher Scientific, Grand Island, NY). A typical yield of ~500 μg of purified mitochondria was obtained per 50 mg sample.

2.9. Respirometry of isolated mitochondria

Isolated mitochondria respirometry was performed using an XF24–3 Extracellular Flux Analyzer (Seahorse Bioscience, North Billerica, MA). The procedure was previously described by Rogers et al. [48] and employed as previously described [36]. During study protocol optimization, respiration driven by complex 1 using pyruvate/malate was compared with respiration driven by complex 2 using succinate/rotenone. Complex 2 driven respiration was consistently higher, similar to previous reports [48]. In order to ensure adequate sample size and standardization, isolated mitochondrial respirometric analyses were performed using succinate and rotenone. Compounds were prepared in 1X MAS at 10X the final concentration required for the assay. Final concentrations of compounds were as follows: ADP, 2 μM oligomycin, 6 μM FCCP, and 2 μM antimycin A. Five μg of the mitochondrial suspension was added to each well and the plate centrifuged at 2000 × *g* at 4 °C for 20 min to ensure attachment. After centrifugation, 450 mL of 1X MAS containing succinate (10 mM) and rotenone (2 μM) was gently added to each well and the experiment initiated. The respirometric assay was performed at 37 °C. Primary outcomes were: maximal State 3 respiration, initiated with ADP (MAX-A), maximal FCCP-linked respiration (MAX), and State 4o, induced by the inhibition of ATP synthase by the addition of oligomycin. The respiratory control ratio (RCR) was calculated as MAX-A/State4o (RCR-A) and MAX/State 4o (RCR-F).

2.10. Statistical analyses

Distributions of all variables were examined before any further analysis. All variables satisfied the normality assumption as assessed using Shapiro-Wilk tests. Associations between all variables were assessed using Pearson correlation coefficients (R) and further separately controlled for age, weight, and HOMA-IR. Correlations are tabulated for each blood cell type analyzed and regression plots between some of the most commonly published variables are depicted following each correlation table. The regression plots we have chosen to show are between MAX respiration of each blood cell type with complex I and complex I+II OXPHOS from permeabilized skeletal muscle fibers as well as FCCP-linked MAX respiration and RCR-F from isolated mitochondria from skeletal muscle and cardiac tissue. The analyses were performed (SPSS v22; Armonk, NY). 95% confidence intervals (95%CI) were generated for the correlation coefficients by bootstrapping.

Table 1
Baseline characteristics of non-human primate subjects enrolled in this study.

	Mean	SD	Range	N
Age (years)	16.6	6.1	8.4–23.7	18
Weight (kg)	4.9	1.0	3.3–6.9	18
BMI (kg/m^2)	60.7	10.5	44.6–82.3	18
Glucose (mg/dL)	127.7	70.6	73.0–319.0	18
Insulin (mIU/L)	23.7	26.7	4.6–114.6	18
HOMA-IR	6.9	7.1	1.0–27.2	18

BMI=body mass index, HOMA-IR=homeostatic model of insulin resistance, SD=standard deviation.
BMI was estimated using trunk length measured from the suprasternal notch to the pubic symphysis.

3. Results

3.1. Demographic and bioenergetic parameters of non-human primate participants

Age, body weight, BMI, insulin, glucose, and homeostatic model assessment of insulin resistance (HOMA-IR) are summarized in Table 1. A total of 18 vervet macaques, all female, were studied with a mean age of 16.4 years. The ages ranged from 8.4 to 23.7 years. The mean weight of the animals was 4.9 kg. Glucose and insulin levels averaged 127.7 mg/dL and 23.7 mIU/L; respectively, with median values of 98.0 mg/dL and 13.5 mIU/L; respectively, indicating wide ranges of variability. The average HOMA-IR was 6.9 with a median of 4.0, indicating some animals to be insulin resistant while others were insulin-sensitive [30]. Representative bioenergetic profiles from each tissue of one animal are shown in Fig. 1, and baseline bioenergetic parameters for each animal are summarized in Table 2.

3.2. Correlations between monocyte blood cell bioenergetics with isolated mitochondria from skeletal and cardiac muscle and permeabilized skeletal muscle fibers

Pearson correlation coefficients were used to compare all blood cell bioenergetic parameters with skeletal and cardiac muscle bioenergetics. The relationships between primary monocyte bioenergetic parameters with skeletal and cardiac muscle bioenergetics are summarized in Table 3 and regression plots depicting these relationships can be found in Fig. 2. Maximal FCCP-linked bioenergetic capacity (MAX) of CD14+ monocytes was significantly positively correlated with permeabilized skeletal muscle maximal oxidative phosphorylation capacity (OXPHOS) driven using substrates for complexes I and II (R=0.75, CI: 0.38–0.97; Fig. 2A) and substrates for complex I alone (R=0.73, CI: 0.33–0.91; Fig. 2B). In addition, basal respiration and reserve capacity of monocytes were significantly correlated with complex I+II and complex I OXPHOS in permeabilized skeletal muscle fibers. Monocyte MAX also significantly positively correlated with the skeletal muscle isolated mitochondrial FCCP-linked respiratory control ratio (RCR-F; R=0.70, CI: 0.35–0.89; Fig. 2D) but not

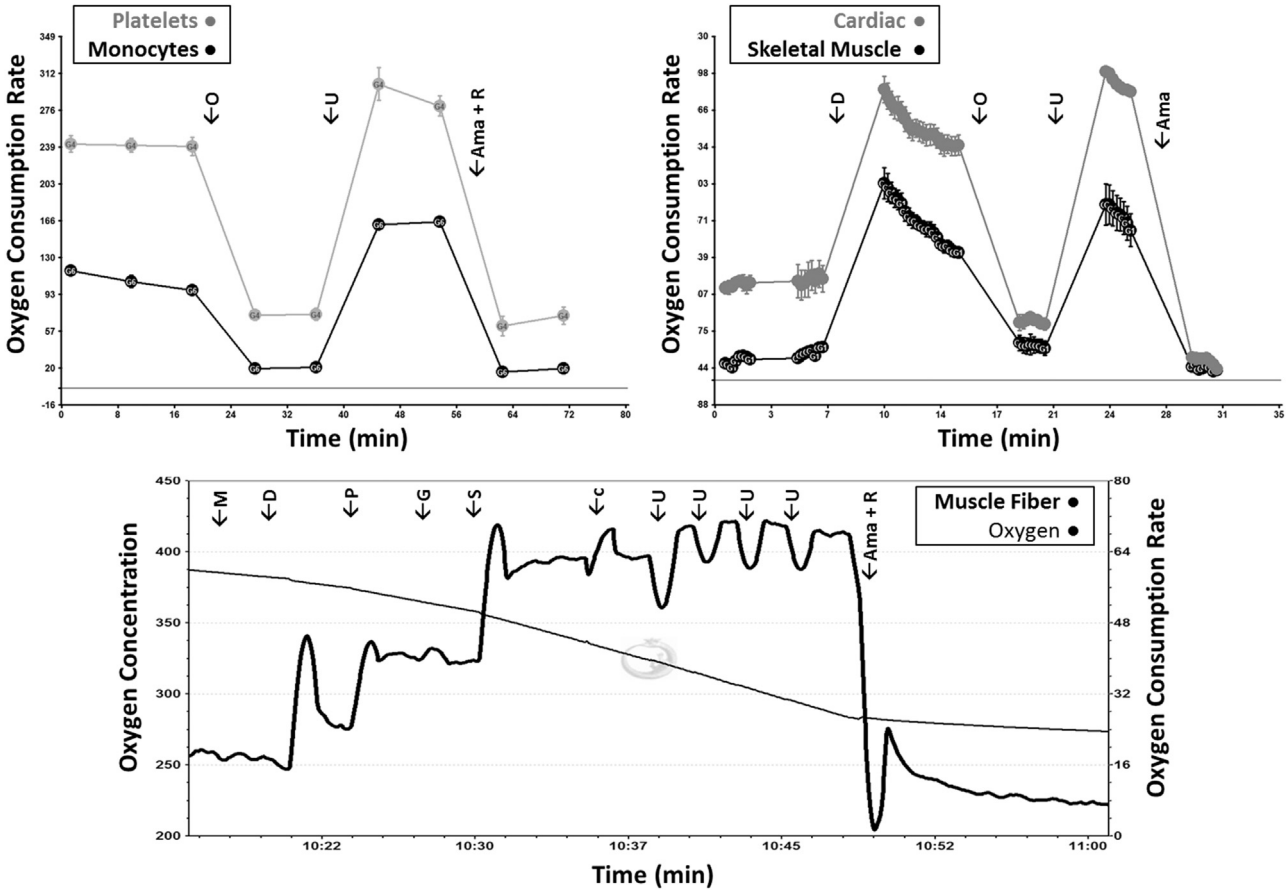

Fig. 1. Representative bioenergetic profiles from CD14+ monocytes, platelets, skeletal muscle isolated mitochondria, cardiac isolated mitochondria, and permeabilized skeletal muscle fibers from one animal. Respiration is measured as oxygen consumption rate (pmol/min/250,000 cells [monocytes], pmol/min/mg protein [platelets], pmol/min/5 μg mitochondrial protein [left vastus and cardiac tissues]), and pmol/min/mg dry weight [permeabilized fibers]. In isolated mitochondrial preparations, complex II (CII) respiration was measured using succinate and rotenone as substrates. Ama=antimycin-A, c=cytochrome c, D=adenosine diphosphate, F=carbonyl-cyanide-p-trifluoromethoxyphenylhydrazone, G=glutamate, M=malate, O=oligomycin, P=pyruvate, R=rotenone, S=succinate, U=uncoupler (FCCP).

Table 2
Baseline bioenergetic characteristics of non-human primate subjects enrolled in this study.

	Mean	SD	Range	N
Platelet basal	299.0	98.8	162.2–435.6	17
Platelet oligomycin OCR	98.3	26.4	54.4–140.4	15
Platelet MAX	438.1	159.8	209.3–699.5	17
Platelet non-mitochondrial OCR	84.4	23.3	36.1–124.4	17
Platelet reserve capacity	139.1	78.5	27.4–263.9	17
Platelet ATP OCR	198.4	77.9	76.8–304.0	15
Platelet leak OCR	12.2	13.5	−7.2 to 39.1	15
Monocyte basal	79.6	37.3	39.3–158.8	11
Monocyte oligomycin OCR	25.2	9.4	13.7–37.3	9
Monocyte MAX	116.2	54.9	50.6–225.3	11
Monocyte non-mitochondrial OCR	19.0	12.7	−8.8 to 37.9	11
Monocyte reserve capacity	36.6	19.6	10.7–66.4	11
Monocyte ATP OCR	48.8	24.8	19.6–86.5	9
Monocyte leak OCR	4.7	10.6	−20.6 to 13.9	9
Permeabilized fiber basal	34.8	9.2	23.4–57.8	17
Permeabilized fiber leak OCR	33.6	12.2	21.0–67.1	17
Permeabilized fiber complex I OXPHOS	93.9	22.7	60.1–145.7	17
Permeabilized fiber complex I+II OXPHOS	133.3	34.4	68.0–197.6	17
Permeabilized fiber cytochrome C membrane integrity	132.7	35.8	63.5–200.3	17
Permeabilized fiber MAX	157.4	33.4	116.8–215.7	17
Permeabilized fiber non-mitochondrial OCR	12.0	3.8	5.1–20.1	17
Left vastus isolated mitochondria CII oligomycin OCR	117.4	50.8	43.0–240.5	16
Left vastus isolated mitochondria CII state 3	581.4	247.9	162.1–1082.1	16
Left vastus isolated mitochondria CII MAX	601.2	292.1	156.6–1062.0	16
Left vastus isolated mitochondria CII RCR-A	5.1	1.4	2.6–8.4	16
Left vastus isolated mitochondria CII RCR-F	5.1	1.5	2.5–7.5	16
Cardiac isolated mitochondria CII oligomycin OCR	162.6	68.2	47.2–268.5	16
Cardiac isolated mitochondria CII state 3	633.4	213.9	171.9–928.4	16
Cardiac isolated mitochondria CII MAX	669.1	225.7	265.6–1052.5	16
Cardiac isolated mitochondria CII RCR-A	4.1	1.0	2.8–6.8	16
Cardiac isolated mitochondria CII RCR-F	4.4	1.1	2.8–7.2	16

ATP=adenosine triphosphate, CII=complex 2, FCCP=Carbonyl cyanide-4-(trifluoromethoxy) phenylhydrazone, MAX=FCCP-linked respiration, OCR=oxygen consumption rate, OXPHOS=oxidative phosphorylation capacity, RCR=respiratory control ratio.
Respiration is measured as oxygen consumption rate (pmol/min/mg protein [platelets], pmol/min/250,000 cells [monocytes], pmol/min/mg dry weight [permeabilized fibers], pmol/min/5 μg mitochondrial protein [left vastus and cardiac tissues]).
In blood cell respiration, Reserve capacity is calculated as the difference between MAX and Basal respiration and Leak is calculated as the difference between Oligo and A/R respiration.
RCRs are calculated as ADP-stimulated State 3 respiration divided by oligomycin-linked respiration (RCR-A) and by MAX respiration divided by oligomycin-linked respiration (RCR-F).
In permeabilized muscle fiber preparations, basal respiration was measured with no added substrates, leak was measured with malate added, complex I OXPHOS capacity was measured using pyruvate, glutamate, and malate with a saturating amount of ADP. Complex I+II OXPHOS capacity was measured using complex I substrates with succinate added. Cytochrome C Membrane Integrity was measured with Complex I+II substrates with cytochrome c added. MAX respiration was measured using complex I+II substrates with FCCP titrations added. Non-mitochondrial respiration was measured with MAX substrates with antimycin-A and rotenone substrates added.
In isolated mitochondrial preparations, CII respiration was measured using succinate and rotenone as substrates and using ADP, oligomycin, and FCCP injections to measure State 3, oligomycin, and MAX, respectively.

Table 3
Relationship between monocyte bioenergetics with skeletal and cardiac muscle bioenergetics. Pearson correlations and 95% confidence intervals of monocyte respiratory parameters with bioenergetics from permeabilized skeletal muscle fibers and isolated mitochondria from *vastus lateralis* and cardiac tissue.

	Basal (95% CI)	MAX (95% CI)	Reserve (95% CI)
Permeabilized fibers:			
Basal	−0.43 (−0.74 to 0.03)	−0.42 (−0.74 to 0.03)	−0.33 (−0.65 to 0.17)
Complex I OXPHOS	**0.74 (0.42–0.91)**	**0.73 (0.33–0.91)**	**0.60 (0.03–0.91)**
Complex I+II OXPHOS	**0.79 (0.49–0.96)**	**0.75 (0.38–0.97)**	**0.57 (0.06–0.92)**
MAX	0.09 (−0.51 to 0.73)	−0.01 (−0.59 to 0.70)	−0.20 (−0.67 to 0.57)
Left vastus CII:			
State 3	−0.24 (−0.73 to 0.55)	−0.24 (−0.79 to 0.63)	−0.23 (−0.86 to 0.67)
MAX	−0.20 (−0.73 to 0.55)	−0.18 (−0.76 to 0.56)	−0.13 (−0.79 to 0.62)
RCR-A	**0.87 (0.58–0.96)**	**0.83 (0.49–0.97)**	**0.69 (0.22–0.98)**
RCR-F	**0.71 (0.30–0.91)**	**0.70 (0.35–0.89)**	**0.62 (0.10–0.89)**
Cardiac CII:			
State 3	0.06 (−0.36 to 0.68)	0.09 (−0.40 to 0.64)	0.14 (−0.45 to 0.64)
MAX	0.16 (−0.29 to 0.85)	0.19 (−0.32 to 0.82)	0.22 (−0.43 to 0.74)
RCR-A	**0.49 (0.14–0.81)**	**0.55 (0.22–0.86)**	**0.58 (0.28–0.87)**
RCR-F	0.52 (−0.21 to 0.98)	0.50 (−0.18 to 0.96)	0.41 (−0.11 to 0.89)

CII=complex 2, FCCP=carbonyl cyanide-4-(trifluoromethoxy)phenylhydrazone, MAX=FCCP-linked respiration, OXPHOS=oxidative phosphorylation capacity, RCR=respiratory control ratio. Bold type = p-value ≤ 0.05.
Respiration is measured as oxygen consumption rate (pmol/min/250,000 cells [monocytes], pmol/min/mg dry weight [permeabilized fibers], pmol/min/5 μg mitochondrial protein [left vastus and cardiac tissues]).
Reserve capacity is calculated as the difference between MAX and Basal respiration.
RCRs are calculated as ADP-stimulated State 3 respiration divided by oligomycin-linked respiration (RCR-A) and by MAX respiration divided by oligomycin-linked respiration (RCR-F).
In permeabilized muscle fiber preparations, basal respiration was measured with no added substrates, leak was measured with malate added, complex I OXPHOS capacity was measured using pyruvate, glutamate, and malate with a saturating amount of ADP. Complex I+II OXPHOS capacity was measured using complex I substrates with succinate added. MAX respiration was measured using complex I+II substrates with FCCP titrations added. Non-mitochondrial respiration was measured with MAX substrates with antimycin-A and rotenone substrates added.
In isolated mitochondrial preparations, CII respiration was measured using succinate and rotenone as substrates and using ADP, oligomycin, and FCCP injections to measure State 3, oligomycin, and MAX respiration, respectively.
N=11–12.

isolated mitochondrial MAX from skeletal or cardiac muscle (Fig. 2C and E). Similarly, a strong positive correlation was found between monocyte MAX with the ADP-linked respiratory control ratio (RCR-A; R=0.83, CI: 0.49–0.97). Monocyte MAX was strongly positively correlated with RCR-A from cardiac muscle isolated mitochondria also (R=0.55, CI: 0.22–0.86).

3.3. Correlations between platelet bioenergetics with isolated mitochondria from skeletal and cardiac muscle and permeabilized skeletal muscle fibers

Correlations of platelet bioenergetic parameters with skeletal and cardiac muscle bioenergetics are summarized in Table 4. Platelet MAX was significantly positively associated with complex I+II OXPHOS in permeabilized skeletal muscle fibers (R=0.51, CI: 0.05–0.81; Fig. 3A). Platelet reserve capacity was associated with complex I+II OXPHOS in permeabilized muscle fibers (R=0.61, CI: 0.22–0.85). Platelet MAX and reserve capacity were also significantly positively correlated with permeabilized skeletal muscle MAX uncoupled respiration (R=0.44, CI: 0.05–0.74; R=0.58, CI: 0.21–0.85; respectively). Like monocyte MAX, platelet MAX was significantly positively correlated with both RCR-F and RCR-A from skeletal muscle isolated mitochondria (R=0.64, CI: 0.23–0.89, Fig. 3D; R=0.53, CI: 0.16–0.83; respectively). Platelet reserve capacity was

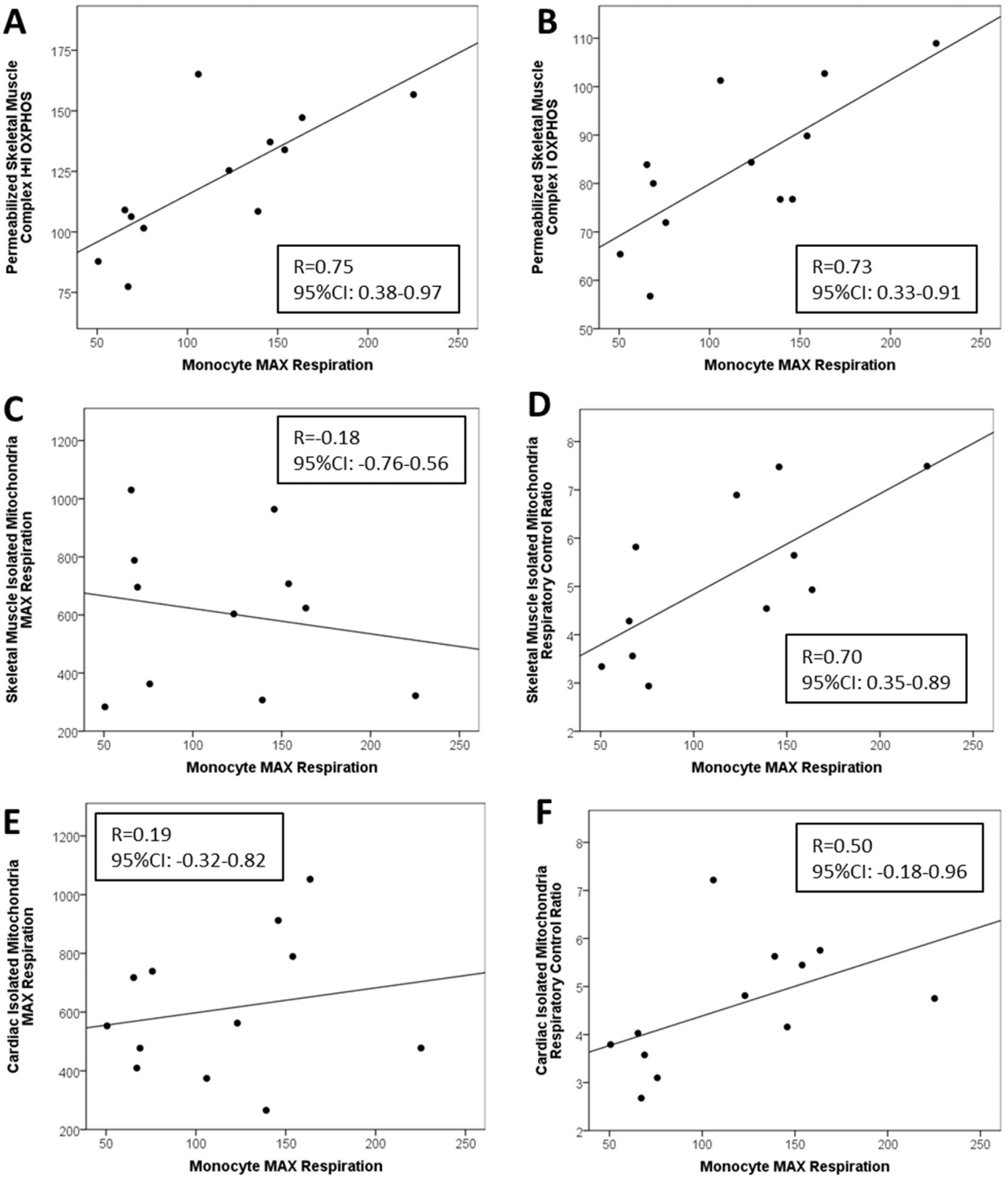

Fig. 2. Associations among CD14+ monocyte bioenergetic parameters with skeletal and cardiac muscle bioenergetics**.** Regressions between monocyte maximal uncoupled respiration and reserve capacity with respiratory control ratio and maximal uncoupled respiration from isolated mitochondria from skeletal and cardiac muscle as well as maximal oxidative phosphorylation capacity and maximal uncoupled respiration from permeabilized skeletal muscle fibers. Pearson's correlations and p-values for each association are shown.

also significantly positively correlated with RCR-F and RCR-A as well as skeletal muscle isolated mitochondrial MAX (R=0.59, CI: 0.18–0.87) and state 3 bioenergetic capacity (R=0.57, CI: 0.17–0.80). In addition, platelet MAX was significantly positively correlated to RCR-F and RCR-A of cardiac isolated mitochondria (R=0.58, CI: 0.22–0.85, Fig. 3F; R=0.42, CI: 0.03–0.80; respectively).

Table 4
Relationship between platelet bioenergetics with skeletal and cardiac muscle bioenergetics. Pearson correlations and 95% confidence intervals of platelet respiratory parameters with bioenergetics from permeabilized skeletal muscle fibers and isolated mitochondria from *vastus lateralis* and cardiac tissue.

	Basal (95% CI)	MAX (95% CI)	Reserve (95% CI)
Permeabilized fibers:			
Basal	−0.06 (−0.53 to 0.42)	0.10 (−0.56 to 0.57)	0.27 (−0.61 to 0.74)
Complex I OXPHOS	0.19 (−0.39 to 0.67)	0.34 (−0.21 to 0.72)	0.45 (−0.04 to 0.79)
Complex I+II OXPHOS	0.34 (−0.25 to 0.81)	**0.51 (0.05–0.81)**	**0.61 (0.22–0.85)**
MAX	0.26 (−0.29 to 0.81)	**0.44 (0.05–0.74)**	**0.58 (0.21–0.88)**
Left vastus CII:			
State 3	0.05 (−0.46 to 0.64)	0.32 (−0.06 to 0.64)	**0.57 (0.17–0.80)**
MAX	0.12 (−0.46 to 0.72)	0.36 (−0.07 to 0.70)	**0.59 (0.18–0.87)**
RCR-A	0.40 (−0.24 to 0.87)	**0.53 (0.16–0.83)**	**0.56 (0.10–0.87)**
RCR-F	0.49 (−0.18 to 0.93)	**0.64 (0.23–0.89)**	**0.69 (0.35–0.90)**
Cardiac CII:			
State 3	−0.26 (−0.66 to 0.29)	−0.08 (−0.53 to 0.47)	0.18 (−0.31 to 0.68)
MAX	−0.16 (−0.61 to 0.41)	0.01 (−0.48 to 0.54)	0.22 (−0.31 to 0.70)
RCR-A	0.35 (−0.04 to 0.74)	**0.42 (0.03–0.80)**	**0.42 (0.07–0.75)**
RCR-F	**0.56 (0.18–0.86)**	**0.58 (0.22–0.85)**	**0.46 (0.03–0.81)**

CII=complex 2, FCCP=carbonyl cyanide-4-(trifluoromethoxy) phenylhydrazone, MAX=FCCP-linked respiration, OXPHOS=oxidative phosphorylation capacity, RCR=respiratory control ratio. Bold type = p-value ≤ 0.05.
Respiration is measured as oxygen consumption rate (pmol/min/mg protein [platelets], pmol/min/mg dry weight [permeabilized fibers], pmol/min/5 μg mitochondrial protein [left vastus and cardiac tissues]).
Reserve capacity is calculated as the difference between MAX and Basal respiration.
RCRs are calculated as ADP-stimulated State 3 respiration divided by oligomycin-linked respiration (RCR-A) and by MAX respiration divided by oligomycin-linked respiration (RCR-F).
In permeabilized muscle fiber preparations, basal respiration was measured with no added substrates, leak was measured with malate added, complex I OXPHOS capacity was measured using pyruvate, glutamate, and malate with a saturating amount of ADP. Complex I+II OXPHOS capacity was measured using complex I substrates with succinate added. MAX respiration was measured using complex I+II substrates with FCCP titrations added. Non-mitochondrial respiration was measured with MAX substrates with antimycin-A and rotenone substrates added.
In isolated mitochondrial preparations, CII respiration was measured using succinate and rotenone as substrates and using ADP, oligomycin, and FCCP injections to measure State 3, oligomycin, and MAX respiration, respectively.
N=16–17.

3.4. Partial correlations between monocyte bioenergetics with isolated mitochondria from skeletal and cardiac muscle and permeabilized skeletal muscle

Partial correlations between monocytes with permeabilized skeletal muscle fibers, independently controlling for age, weight, and HOMA-IR, are summarized in Table 5. When controlled for weight, correlations between monocyte cellular respiration with permeabilized skeletal muscle complex I+II OXPHOS were no longer statistically significant, indicating a possible interaction between bioenergetic function with weight (Table 5). The statistically significant relationships between monocyte respiration with isolated mitochondria from skeletal muscle were weakened after controlling for age, weight, and HOMA-IR for RCR-F. Controlling for weight reduced the strength of the associations between monocyte reserve capacity with complex I and I+II OXPHOS, and isolated skeletal muscle mitochondrial RCR-F and RCR-A. The only relationship that persisted between monocyte bioenergetics with cardiac isolated mitochondria was between monocyte reserve capacity and RCR-A when controlling for weight (Table 6).

3.5. Partial correlations between platelet bioenergetics with isolated mitochondria from skeletal and cardiac muscle and permeabilized skeletal muscle

Partial correlations between platelets with isolated mitochondria from skeletal and cardiac muscle and permeabilized skeletal muscle fibers, independently controlling for age, weight, and HOMA-IR, are summarized in Table 5. Platelet reserve capacity significantly positively correlated with permeabilized skeletal muscle complex I+II OXPHOS and MAX uncoupled respiration after independently controlling for age, weight, and HOMA-IR using partial correlations (Table 5). Relationships between cardiac isolated mitochondria were weakened except platelet reserve remained correlated with RCR-A when controlling for weight and platelet basal, MAX, and reserve positively correlated with RCR-F when controlling for HOMA-IR (Table 7).

4. Discussion

Mitochondrial dysfunction is a primary driver of many diseases, particularly chronic pathologies associated with aging, including obesity [47], diabetes [24], and heart failure [25]. Mitochondrial dysfunction may be mediated by various mechanisms such as aberrant mitophagy [12], oxidative stress [49,50], or mitochondrial DNA heteroplasmy [51]. The cumulative effects of defects in these pathways ultimately affect mitochondrial oxidative phosphorylation, which can be assessed by analyzing the oxygen consumption rate of cells or isolated mitochondria [52].

Muscle mitochondrial bioenergetics has been highlighted to play a role in diverse diseases and disorders such as obesity, diabetes, and sarcopenia [53–55]. While muscle respirometry has significantly advanced our mechanistic understanding of mitochondrial bioenergetics, such measures may present undue burden in large scale clinical trials, or studies focused on patients with contraindications to biopsy, such as more frail older adults. In recent years, the potential relationships between mitochondrial function measured in blood cells with various disease states and disorders has gained attention [56]. This study directly addresses whether the bioenergetic profile of circulating cells are related to key aspects of mitochondrial function measured in skeletal and cardiac muscle. The primary finding we report is that blood cell maximal respiration is positively correlated with multiple measures of oxidative capacity in permeabilized muscle fiber bundles. The respiratory capacities of intact blood cells and muscle fibers both incorporate the cumulative effects of intrinsic OXPHOS capacity and mitochondrial content on overall bioenergetic capacity. Interestingly, we also found that the maximal respiratory capacity of monocytes and platelets are

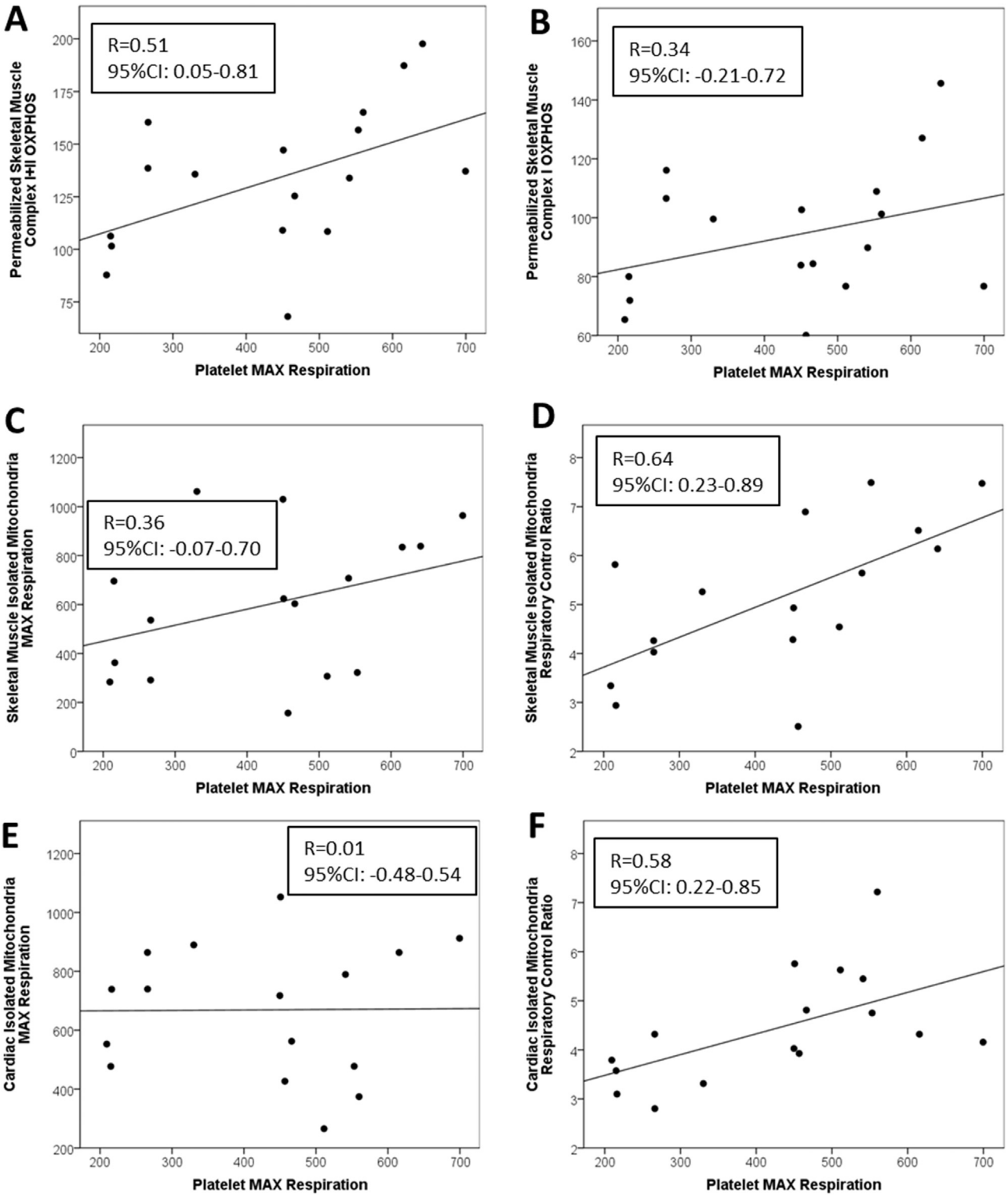

Fig. 3. Associations among platelet bioenergetic parameters with skeletal and cardiac muscle bioenergetics. Regressions between platelet maximal uncoupled respiration and reserve capacity with respiratory control ratio and maximal uncoupled respiration from isolated mitochondria from skeletal and cardiac muscle as well as maximal oxidative phosphorylation capacity and maximal uncoupled respiration from permeabilized skeletal muscle fibers. Pearson's correlations and p-values for each association are shown.

associated with respiratory control, a reliable measure of mitochondrial coupling, measured in isolated skeletal and cardiac muscle mitochondria [57]. These results suggest that blood cell respiration is related to differences in overall bioenergetic function, taking into account potential differences in mitochondrial content and networking activity, as well as intrinsic ETC function. Overall, the findings reported in this manuscript support the hypothesis that blood cell respirometry can recapitulate key readouts of systemic bioenergetic capacity and provide a minimally-invasive index of muscle metabolic health. Future longitudinal studies are required in order to determine how bioenergetic capacity changes across tissues with time and with disease onset/progression.

Table 5
Partial correlations between monocyte and platelet bioenergetics with permeabilized skeletal muscle bioenergetics. Partial correlations and 95% confidence intervals of monocyte and platelet respiratory parameters with bioenergetics from permeabilized skeletal muscle fibers left *vastus lateralis*, controlling for age, weight, and insulin status.

	Partial (age)			**Partial (weight)**			**Partial (HOMA-IR)**		
Permeabilized fibers:	**Basal (95% CI)**	**MAX (95% CI)**	**Reserve (95% CI)**	**Basal (95% CI)**	**MAX (95% CI)**	**Reserve (95% CI)**	**Basal (95% CI)**	**MAX (95% CI)**	**Reserve (95% CI)**
Monocytes:									
Basal	**−0.55 (−0.83 to −0.17)**	−0.49 (−0.82 to 0.03)	−0.36 (−0.79 to 0.42)	**−0.47 (−0.79 to −0.14)**	**−0.46 (−0.79 to −0.09)**	−0.38 (−0.78 to 0.22)	**−0.51 (−0.85 to −0.04)**	−0.50 (−0.83 to 0.12)	−0.43 (−0.76 to 0.30)
Complex I OXPHOS	**0.64 (0.13–0.89)**	**0.63 (0.13–0.90)**	0.56 (−0.11 to 0.90)	**0.76 (0.26–0.92)**	**0.75 (0.26–0.92)**	0.63 (−0.03 to 0.91)	**0.74 (0.16–0.95)**	**0.73 (0.13–0.95)**	0.61 (−0.15 to 0.91)
Complex I+II OXPHOS	**0.71 (0.26–0.96)**	**0.67 (0.02–0.97)**	0.52 (−0.30 to 0.95)	0.79 (−0.30 to 0.97)	0.75 (−0.28 to 0.98)	0.57 (−0.42 to 0.93)	**0.79 (0.39–0.98)**	**0.75 (0.34–0.97)**	0.57 (−0.03 to 0.91)
MAX	−0.19 (−0.72 to 0.56)	−0.27 (−0.77 to 0.52)	−0.37 (−0.81 to 0.40)	0.21 (−0.63 to 0.86)	0.12 (−0.85 to 0.69)	−0.07 (−0.77 to 0.66)	0.06 (−0.57 to 0.76)	−0.05 (−0.64−0.68)	−0.25 (−0.81−0.47)
Platelets:									
Basal	−0.25 (−0.72 to 0.34)	−0.04 (−0.59 to 0.51)	0.21 (−0.40 to 0.69)	−0.07 (−0.71 to 0.32)	0.07 (−0.58 to 0.47)	0.25 (−0.40 to 0.63)	−0.11 (−0.51 to 0.35)	0.06 (−0.42 to 0.48)	0.25 (−0.43 to 0.70)
Complex I OXPHOS	0.18 (−0.40 to 0.69)	0.34 (−0.22 to 0.78)	0.08 (−0.14 to 0.79)	0.19 (−0.39 to 0.60)	0.34 (−0.20 to 0.66)	0.46 (−0.09 to 0.79)	0.14 (−0.48 to 0.60)	0.30 (−0.27 to 0.65)	0.43 (−0.15 to 0.74)
Complex I+II OXPHOS	0.34 (−0.16 to 0.83)	0.52 (−0.11 to 0.84)	**0.60 (0.13–0.84)**	0.34 (−0.27 to 0.81)	0.52 (0.11–0.78)	**0.62 (0.19–0.84)**	0.31 (−0.31 to 0.79)	0.50 (0.01–0.79)	**0.60 (0.19–0.82)**
MAX	0.17 (−0.36 to 0.68)	0.40 (−0.05 to 0.76)	**0.56 (0.12–0.88)**	0.25 (−0.36 to 0.67)	0.43 (−0.05 to 0.73)	**0.57 (0.15–0.83)**	0.25 (−0.29 to 0.67)	0.46 (−0.02 to 0.75)	**0.59 (0.18–0.85)**

FCCP=carbonyl cyanide-4-(trifluoromethoxy) phenylhydrazone, HOMA-IR=homeostatic model of insulin resistance, MAX=FCCP-linked respiration, OXPHOS=oxidative phosphorylation capacity. Bold type = p-value ≤ 0.05.
Respiration is measured as oxygen consumption rate (pmol/min/mg protein [platelets], pmol/min/250,000 cells [monocytes], and pmol/min/mg dry weight [permeabilized fibers]).
Reserve capacity is calculated as the difference between MAX and Basal respiration.
In permeabilized muscle fiber preparations, basal respiration was measured with no added substrates, leak was measured with malate added, complex I OXPHOS capacity was measured using pyruvate, glutamate, and malate with a saturating amount of ADP. Complex I+II OXPHOS capacity was measured using complex I substrates with succinate added. MAX respiration was measured using complex I+II substrates with FCCP titrations added. Non-mitochondrial respiration was measured with MAX with antimycin-A and rotenone substrates added.
Monocytes: N=12. Platelets: N=17.

Table 6
Partial correlations between monocyte bioenergetics with skeletal and cardiac muscle bioenergetics. Partial correlations and 95% confidence intervals of monocyte respiratory parameters with bioenergetics from isolated mitochondria from left *vastus lateralis* and cardiac tissue, controlling for age, weight, and insulin status.

	Partial (age)			Partial (weight)			Partial (HOMA-IR)		
	Basal (95% CI)	MAX (95% CI)	Reserve (95% CI)	Basal (95% CI)	MAX (95% CI)	Reserve (95% CI)	Basal (95% CI)	MAX (95% CI)	Reserve (95% CI)
Left vastus CII:									
State 3	−0.45 (−0.94 to 0.85)	−0.43 (−0.94 to 0.92)	−0.34 (−0.94 to 0.85)	−0.19 (−0.81 to 0.29)	−0.19 (−0.80 to 0.22)	−0.17 (−0.74 to 0.15)	−0.37 (−0.87 to 0.68)	−0.39 (−0.87 to 0.59)	−0.39 (−0.91 to 0.54)
MAX	−0.22 (−0.90 to 0.90)	−0.19 (−0.87 to 0.93)	−0.13 (−0.88 to 0.92)	−0.18 (−0.78 to 0.37)	−0.16 (−0.76 to 0.26)	−0.11 (−0.68 to 0.24)	−0.37 (−0.88 to 0.71)	−0.37 (−0.91 to 0.76)	−0.33 (−0.95 to 0.74)
RCR-A	**0.80 (0.32–0.97)**	**0.78 (0.29–0.98)**	**0.65 (0.03–0.97)**	**0.86 (0.37–0.97)**	**0.83 (0.36–0.97)**	0.67 (−0.11 to 0.98)	**0.89 (0.57–0.98)**	**0.84 (0.45–0.98)**	**0.65 (0.02–0.99)**
RCR-F	**0.74 (0.33–0.93)**	**0.72 (0.28–0.95)**	0.61 (−0.15 to 0.95)	**0.68 (0.14–0.92)**	**0.67 (0.09–0.89)**	0.58 (−0.25 to 0.84)	0.73 (−0.36 to 0.99)	0.71 (−0.15 to 0.99)	**0.59 (0.04–0.96)**
Cardiac CII:									
State 3	0.06 (−0.55 to 0.80)	0.10 (−0.55 to 0.74)	0.14 (−0.63 to 0.69)	0.13 (−0.42 to 0.82)	0.18 (−0.47 to 0.89)	0.26 (−0.51 to 0.82)	0.11 (−0.47 to 0.76)	0.16 (−0.50 to 0.82)	0.22 (−0.67 to 0.85)
MAX	0.17 (−0.44 to 0.90)	0.20 (−0.43 to 0.87)	0.22 (−0.50 to 0.81)	0.22 (−0.34 to 0.83)	0.26 (−0.46 to 0.88)	0.31 (−0.60 to 0.89)	0.24 (−0.26 to 0.78)	0.29 (−0.35 to 0.85)	0.33 (−0.61 to 0.90)
RCR-A	0.32 (−0.40 to 0.90)	0.42 (−0.32 to 0.91)	0.53 (−0.05 to 0.87)	0.53 (−0.33 to 0.91)	0.61 (−0.10 to 0.94)	**0.66 (0.27–0.97)**	0.45 (−0.27 to 0.93)	0.51 (−0.18 to 0.98)	0.54 (−0.53 to 0.99)
RCR-F	0.36 (−0.77–0.93)	0.36 (−0.78 to 0.94)	0.33 (−0.77 to 0.92)	0.57 (−0.44 to 0.96)	0.57 (−0.51 to 0.97)	0.48 (−0.39 to 0.95)	0.52 (−0.01 to 0.96)	0.51 (−0.26 to 0.97)	0.42 (−0.37 to 0.92)

CII=complex 2, FCCP=carbonyl cyanide-4-(trifluoromethoxy) phenylhydrazone, HOMA-IR=homeostatic model of insulin resistance, MAX=FCCP-linked respiration, OXPHOS=oxidative phosphorylation capacity, RCR=respiratory control ratio. Bold type = p-value ≤ 0.05.
Respiration is measured as oxygen consumption rate (pmol/min/250,000 cells [monocytes] and pmol/min/5 μg mitochondrial protein [left vastus and cardiac tissues]).
Reserve capacity is calculated as the difference between MAX and Basal respiration.
RCRs are calculated as ADP-stimulated State 3 respiration divided by oligomycin-linked respiration (RCR-A) and by MAX respiration divided by oligomycin-linked respiration (RCR-F).
In isolated mitochondrial preparations, CII respiration was measured using succinate and rotenone as substrates and using ADP, oligomycin, and FCCP injections to measure State 3, oligomycin, and MAX respiration, respectively.
N=11–12.

The comparison of blood based bioenergetic profiles with respiratory analyses of both permeabilized muscle fibers and isolated mitochondria from freshly isolated tissues in a well phenotyped non-human primate model with high variability in age and metabolic health are major strengths of the present study. Kavanagh et al. have studied metabolically healthy and unhealthy female vervet macaques and have published mean values for glucose (60.5 mg/dL and 104.7 mg/dL; respectively), insulin (20.8 mIU/mL and 26.5 mIU/mL; respectively), and HOMA-IR (3.04 and 6.76; respectively). These values are similar to those measured from our cohort over the same range of ages, although the variability is greater in the metabolically diverse cohort of animals used for this study [30]. The oxygen consumption rates published by Chacko et al. for monocytes (83.9 pmol/min/250k cells) and platelets (199.4 pmol/min/25million cells) are similar to what was measured in our study, and permeabilized fibers from non-human primates are similar to results from humans published by others [41,58]. Similarly, respiratory control ratios of isolated skeletal and cardiac muscle are similar to those described in human cardiac and skeletal muscle by Park et al. (5.3 ± 0.7, 3.2 ± 0.4) and others [59–61]. Altogether, we believe that the respiration rates we report in this study are in line with previous reports by other groups.

It should be noted that fundamental methodological differences exist when measuring mitochondrial function in different tissues and circulating cells. This limits the comparisons that can logically be made a between the various readouts we report. Blood cells were kept intact for respirometric assessments; however, skeletal muscle fibers are permeabilized with a mild detergent, specific for cholesterol esters found predominantly in the plasma membrane but not mitochondrial membranes [62]. Isolated mitochondrial preparations utilized in this study focus on intrinsic ETC properties, without potential input from non-mitochondrial contributors to respiratory capacity or differences in mitochondrial content. Taking these methodological differences into consideration, the most straightforward comparison that can be made is between the respiratory capacities of blood cells and muscle fibers. Indeed, we find that these measures are significantly positively correlated, even after controlling for multiple covariates. For comparisons between the respiratory capacity of intact blood cells with isolated muscle mitochondria, we believe that RCR represents an appropriate measure of intrinsic ETC function. It has been proposed by Brand and Nicholls that RCR is a reliable measure of function when using isolated mitochondria because it is highly tissue- and substrate-dependent and changes with any alteration in oxidative phosphorylation [57]. The relationships between monocyte and platelet respiration with the RCR of the isolated mitochondria suggests that higher overall respiration in blood cells may also be related to the intrinsic coupling of the mitochondria, regardless of mitochondrial content within the muscle. Future studies using permeabilized blood cells and isolated blood cell mitochondria may help to clarify these relationships. A limitation of this study is that we report data only for complex II driven respiration in the isolated mitochondrial preparations. Future studies should compare both complex I and complex II driven respiration in isolated mitochondria as well as permeabilized blood cells.

It is clear that a range of diseases manifest with alterations in mitochondrial function; whether they are of genetic mitochondrial etiology, acute disruptions such as ischemia reperfusion, or chronic as is the case with many diseases associated with aging. It was recently demonstrated that basal and maximal bioenergetic function measured in monocytes is reduced post-operatively compared with healthy controls [63]. It was also shown that patients with diabetic nephropathy have reduced reserve capacity and maximal respiration in peripheral blood mononuclear cells with evidence that elevated circulating mitochondrial DNA may

Table 7
Partial correlations between platelet bioenergetics with skeletal and cardiac muscle bioenergetics. Partial correlations and 95% confidence intervals of platelet respiratory parameters with bioenergetics from isolated mitochondria from left *vastus lateralis* and cardiac tissue, controlling for age, weight, and insulin status.

	Partial (age)			**Partial (weight)**			**Partial (HOMA-IR)**		
	Basal (95% CI)	**MAX (95% CI)**	**Reserve (95% CI)**	**Basal (95% CI)**	**MAX (95% CI)**	**Reserve (95% CI)**	**Basal (95% CI)**	**MAX (95% CI)**	**Reserve (95% CI)**
Left vastus CII:									
State 3	0.05 (−0.52 to 0.67)	0.34 (−0.02 to 0.69)	**0.59 (0.20–0.85)**	0.03 (−0.68 to 0.55)	0.30 (−0.32 to 0.62)	**0.57 (0.07–0.80)**	−0.02 (−0.54 to 0.59)	0.28 (−0.13 to 0.66)	**0.56 (0.10–0.84)**
MAX	0.26 (−0.32 to 0.75)	0.51 (0.11–0.81)	**0.67 (0.29–0.92)**	0.10 (−0.61 to 0.59)	0.35 (−0.24 to 0.67)	**0.58 (0.12–0.84)**	0.02 (−0.52 to 0.62)	0.30 (−0.18 to 0.74)	**0.55 (0.05–0.90)**
RCR-A	0.23 (−0.27 to 0.83)	**0.42 (0.04–0.81)**	**0.53 (0.03–0.83)**	0.43 (−0.19 to 0.85)	**0.58 (0.18–0.86)**	**0.63 (0.21–0.89)**	0.29 (−0.31 to 0.84)	**0.44 (0.00–0.80)**	0.51 (−0.05 to 0.84)
RCR-F	0.56 (0.08–0.93)	**0.70 (0.39–0.91)**	**0.71 (0.37–0.92)**	0.50 (−0.09 to 0.93)	**0.67 (0.29–0.91)**	**0.73 (0.45–0.91)**	0.36 (−0.25 to 0.91)	**0.55 (0.08–0.86)**	**0.64 (0.25–0.86)**
Cardiac CII:									
State 3	−0.27 (−0.68 to 0.28)	−0.05 (−0.53 to 0.44)	0.21 (−0.25 to 0.65)	−0.26 (−0.60 to 0.11)	−0.08 (−0.46 to 0.31)	0.18 (−0.21 to 0.53)	−0.24 (−0.70 to 0.40)	−0.04 (−0.58 to 0.54)	0.23 (−0.30 to 0.70)
MAX	−0.13 (−0.61 to 042)	0.06 (−0.48 to 0.55)	0.26 (−0.23 to 067)	−0.16 (−0.53 to 0.21)	0.01 (−0.41 to 0.37)	0.22 (−0.21 to 0.58)	−0.10 (−0.60 to 0.40)	0.08 (−0.48 to 0.55)	0.30 (−0.24 to 0.71)
RCR-A	0.16 (−0.49 to 0.60)	0.29 (−0.41 to 0.71)	0.34 (−0.28 to 0.77)	0.35 (−0.16 to 0.71)	0.43 (−0.13 to 0.84)	**0.42 (0.01–0.77)**	0.29 (−0.36 to 0.74)	0.37 (−0.27 to 0.84)	0.37 (−0.15 to 0.79)
RCR-F	0.46 (−0.01 to 0.78)	0.49 (−0.02 to 0.80)	0.39 (−0.10 to 0.73)	0.56 (−0.10 to 0.90)	0.58 (−0.09 to 0.87)	0.46 (−0.07 to 0.80)	**0.60 (0.21–0.84)**	**0.62 (0.24–0.88)**	**0.48 (0.08–0.80)**

CII = complex 2, FCCP = carbonyl cyanide-4-(trifluoromethoxy) phenylhydrazone, HOMA-IR = homeostatic model of insulin resistance, MAX = FCCP-linked respiration, OXPHOS = oxidative phosphorylation capacity, RCR = respiratory control ratio. Bold type = p-value $\leq$ 0.05.
Respiration is measured as oxygen consumption rate (pmol/min/mg protein [platelets] and pmol/min/5 μg mitochondrial protein [left vastus and cardiac tissues]).
Reserve capacity is calculated as the difference between MAX and Basal respiration.
RCRs are calculated as ADP-stimulated State 3 respiration divided by oligomycin-linked respiration (RCR-A) and by MAX respiration divided by oligomycin-linked respiration (RCR-F).
In isolated mitochondrial preparations, CII respiration was measured using succinate and rotenone as substrates and using ADP, oligomycin, and FCCP injections to measure State 3, oligomycin, and MAX respiration, respectively.
N = 16.

precede the dysfunction in cellular metabolism [64,65]. Here we demonstrate that blood based cellular respirometry is correlated with bioenergetic measures generated by two common methods for measuring skeletal muscle respirometry. These findings, suggest potential applications in future clinical trials and the development of reliable mitochondrial diagnostics. Monocyte and platelet cellular respiration correlated with both skeletal and cardiac muscle respiration. Platelet isolation is easy, quick, and can reliably produce a high yield, making these cells a strong candidate for future development as a clinical diagnostic tool. Future work to compare the reliability of bioenergetic measurements among various blood cell populations is still required, and future studies should investigate the effects of specific circulating factors such as circulating mtDNA, redox stress, cytokines, and other possible mitochondrial damage associated molecular patterns on bioenergetic function of blood cells. In addition, it remains to be determined how blood cell bioenergetics are altered under various disease states common to aging, and how they are affected by interventions that promote healthy aging, including weight loss and exercise.

Funding

This work was supported by the National Institutes of Health, United States [P30-AG21332, P30-AG049638, R21-AG051077, RR019963/OD010965]; and the Department of Veterans Affairs, United States [VA 247-P-0447].

Disclosures

No conflicts of interest, financial or otherwise, are declared by the authors.

Author contributions

D.J.T., M.S.B., T.C.R., and A.J.A.M. planned the study. D.J.T. performed isolations and respirometry of blood cells and skeletal muscle fibers. M.S.B. performed mitochondrial isolations and respirometry of isolated mitochondria. D.J.T. and M.S.B. analyzed results. D.J.T. and A.J.A.M. wrote the manuscript along with M.S.B., M.J.J., and T.C.R.

Acknowledgments

We thank Heather Gregory, John Stone, Tara Chavanne, Margaret Long and Karin Murphy for their help collecting and transporting samples and for helping with respirometry, and we thank Edward Ip, Ph.D for his input on statistical methods.

References

[1] A.M. Japiassu, A.P. Santiago, J.C. d'Avila, L.F. Garcia-Souza, A. Galina, H.C. Castro Faria-Neto, F.A. Bozza, M.F. Oliveira, Bioenergetic failure of human peripheral blood monocytes in patients with septic shock is mediated by reduced F1Fo adenosine-5′-triphosphate synthase activity, Crit. Care Med. 39 (5) (2011) 1056–1063.
[2] S. Zharikov, S. Shiva, Platelet mitochondrial function: from regulation of thrombosis to biomarker of disease, Biochem. Soc. Trans. 41 (1) (2013) 118–123.
[3] S.H. Caldwell, R.H. Swerdlow, E.M. Khan, J.C. Iezzoni, E.E. Hespenheide, J. K. Parks, W.D. Parker Jr., Mitochondrial abnormalities in non-alcoholic steatohepatitis, J. Hepatol. 31 (3) (1999) 430–434.
[4] A.H. Schapira, M. Gu, J.W. Taanman, S.J. Tabrizi, T. Seaton, M. Cleeter, J. M. Cooper, Mitochondria in the etiology and pathogenesis of Parkinson's disease, Ann. Neurol. 44 (3 Suppl 1) (1998) S89–S98.
[5] O. Miro, S. Lopez, E. Martinez, E. Pedrol, A. Milinkovic, E. Deig, G. Garrabou, J. Casademont, J.M. Gatell, F. Cardellach, Mitochondrial effects of HIV infection on the peripheral blood mononuclear cells of HIV-infected patients who were never treated with antiretrovirals, Clin. Infect. Dis. 39 (5) (2004) 710–716.

[6] F. Sjovall, S. Morota, M.J. Hansson, H. Friberg, E. Gnaiger, E. Elmer, Temporal increase of platelet mitochondrial respiration is negatively associated with clinical outcome in patients with sepsis, Crit. Care 14 (6) (2010) R214.
[7] M. Mancuso, D. Orsucci, A. LoGerfo, V. Calsolaro, G. Siciliano, Clinical features and pathogenesis of Alzheimer's disease: involvement of mitochondria and mitochondrial DNA, Adv. Exp. Med. Biol. 685 (2010) 34–44.
[8] C. Avila, R.J. Huang, M.V. Stevens, A.M. Aponte, D. Tripodi, K.Y. Kim, M.N. Sack, Platelet mitochondrial dysfunction is evident in type 2 diabetes in association with modifications of mitochondrial anti-oxidant stress proteins, Exp. Clin. Endocrinol. Diabetes 120 (4) (2012) 248–251.
[9] M.L. Hartman, O.S. Shirihai, M. Holbrook, G. Xu, M. Kocherla, A. Shah, J. L. Fetterman, M.A. Kluge, A.A. Frame, N.M. Hamburg, J.A. Vita, Relation of mitochondrial oxygen consumption in peripheral blood mononuclear cells to vascular function in type 2 diabetes mellitus, Vasc. Med. 19 (1) (2014) 67–74.
[10] M.E. Widlansky, J. Wang, S.M. Shenouda, T.M. Hagen, A.R. Smith, T. J. Kizhakekuttu, M.A. Kluge, D. Weihrauch, D.D. Gutterman, J.A. Vita, Altered mitochondrial membrane potential, mass, and morphology in the mononuclear cells of humans with type 2 diabetes, Transl. Res. 156 (1) (2010) 15–25.
[11] C. Shi, K. Guo, D.T. Yew, Z. Yao, E.L. Forster, H. Wang, J. Xu, Effects of ageing and Alzheimer's disease on mitochondrial function of human platelets, Exp. Gerontol. 43 (6) (2008) 589–594.
[12] M.D. Cordero, M.M. de, A.M. Moreno Fernandez, I.M. Carmona Lopez, M. J. Garrido, D. Cotan, I.L. Gomez, P. Bonal, F. Campa, P. Bullon, P. Navas, J. A. Sanchez Alcazar, Mitochondrial dysfunction and mitophagy activation in blood mononuclear cells of fibromyalgia patients: implications in the pathogenesis of the disease, Arthritis Res. Ther. 12 (1) (2010) R17.
[13] M. Rao, L. Li, C. Demello, D. Guo, B.L. Jaber, B.J. Pereira, V.S. Balakrishnan, Mitochondrial DNA injury and mortality in hemodialysis patients, J. Am. Soc. Nephrol. 20 (1) (2009) 189–196.
[14] O. Miro, S. Lopez, E. Pedrol, B. Rodriguez-Santiago, E. Martinez, A. Soler, A. Milinkovic, J. Casademont, V. Nunes, J.M. Gatell, F. Cardellach, Mitochondrial DNA depletion and respiratory chain enzyme deficiencies are present in peripheral blood mononuclear cells of HIV-infected patients with HAART-related lipodystrophy, Antivir. Ther. 8 (4) (2003) 333–338.
[15] B. Thyagarajan, R. Wang, H. Nelson, H. Barcelo, W.P. Koh, J.M. Yuan, Mitochondrial DNA copy number is associated with breast cancer risk, PLoS One 8 (6) (2013) e65968.
[16] P. Xia, H.X. An, C.X. Dang, R. Radpour, C. Kohler, E. Fokas, R. Engenhart-Cabillic, W. Holzgreve, X.Y. Zhong, Decreased mitochondrial DNA content in blood samples of patients with stage I breast cancer, BMC Cancer 9 (2009) 454.
[17] D. Krige, M.T. Carroll, J.M. Cooper, C.D. Marsden, A.H. Schapira, Platelet mitochondrial function in Parkinson's disease. The Royal Kings and Queens Parkinson Disease Research Group, Ann. Neurol. 32 (6) (1992) 782–788.
[18] C.M. Chen, Y.R. Wu, M.L. Cheng, J.L. Liu, Y.M. Lee, P.W. Lee, B.W. Soong, D. T. Chiu, Increased oxidative damage and mitochondrial abnormalities in the peripheral blood of Huntington's disease patients, Biochem. Biophys. Res. Commun. 359 (2) (2007) 335–340.
[19] D.J. Tyrrell, M.S. Bharadwaj, C.G. Van Horn, S.B. Kritchevsky, B.J. Nicklas, A. J. Molina, Respirometric profiling of muscle mitochondria and blood cells are associated with differences in gait speed among community-dwelling older adults, J. Gerontol. A Biol. Sci. Med. Sci. (2014).
[20] D.J. Tyrrell, M.S. Bharadwaj, C.G. Van Horn, A.P. Marsh, B.J. Nicklas, A.J. Molina, Blood-cell bioenergetics are associated with physical function and inflammation in overweight/obese older adults, Exp. Gerontol. 70 (2015) 84–91.
[21] A. Karabatsiakis, C. Bock, J. Salinas-Manrique, S. Kolassa, E. Calzia, D.E. Dietrich, I.T. Kolassa, Mitochondrial respiration in peripheral blood mononuclear cells correlates with depressive subsymptoms and severity of major depression, Transl. Psychiatry 4 (2014) e397.
[22] K.R. Short, M.L. Bigelow, J. Kahl, R. Singh, J. Coenen-Schimke, S. Raghavakaimal, K.S. Nair, Decline in skeletal muscle mitochondrial function with aging in humans, Proc. Natl. Acad. Sci. USA 102 (15) (2005) 5618–5623.
[23] M. Diamant, H.J. Lamb, Y. Groeneveld, E.L. Endert, J.W. Smit, J.J. Bax, J. A. Romijn, R.A. de, J.K. Radder, Diastolic dysfunction is associated with altered myocardial metabolism in asymptomatic normotensive patients with well-controlled type 2 diabetes mellitus, J. Am. Coll. Cardiol. 42 (2) (2003) 328–335.
[24] E.J. Anderson, A.P. Kypson, E. Rodriguez, C.A. Anderson, E.J. Lehr, P.D. Neufer, Substrate-specific derangements in mitochondrial metabolism and redox balance in the atrium of the type 2 diabetic human heart, J. Am. Coll. Cardiol. 54 (20) (2009) 1891–1898.
[25] D. Montaigne, X. Marechal, A. Coisne, N. Debry, T. Modine, G. Fayad, C. Potelle, J.M. El Arid, S. Mouton, Y. Sebti, H. Duez, S. Preau, I. Remy-Jouet, F. Zerimech, M. Koussa, V. Richard, R. Neviere, J.L. Edme, P. Lefebvre, B. Staels, Myocardial contractile dysfunction is associated with impaired mitochondrial function and dynamics in type 2 diabetic but not in obese patients, Circulation 130 (7) (2014) 554–564.
[26] R.G. Hansford, Bioenergetics in aging, Biochim. Biophys. Acta 726 (1) (1983) 41–80.
[27] K.C. Shekar, L. Li, E.R. Dabkowski, W. Xu, R.F. Ribeiro Jr., P.A. Hecker, F. A. Recchia, R.G. Sadygov, B. Willard, T. Kasumov, W.C. Stanley, Cardiac mitochondrial proteome dynamics with heavy water reveals stable rate of mitochondrial protein synthesis in heart failure despite decline in mitochondrial oxidative capacity, J. Mol. Cell. Cardiol. 75C (2014) 88–97.
[28] X.T. Tigno, G. Gerzanich, B.C. Hansen, Age-related changes in metabolic parameters of nonhuman primates, J. Gerontol. A Biol. Sci. Med. Sci. 59 (11) (2004) 1081–1088.
[29] C.A. Shively, S.L. Willard, T.C. Register, A.J. Bennett, P.J. Pierre, M. L. Laudenslager, D.W. Kitzman, M.K. Childers, R.W. Grange, S.B. Kritchevsky, Aging and physical mobility in group-housed old world monkeys, Age 34 (5) (2012) 1123–1131.
[30] K. Kavanagh, L.A. Fairbanks, J.N. Bailey, M.J. Jorgensen, M. Wilson, L. Zhang, L. L. Rudel, J.D. Wagner, Characterization and heritability of obesity and associated risk factors in vervet monkeys, Obesity 15 (7) (2007) 1666–1674.
[31] J.E. Wagner, K. Kavanagh, G.M. Ward, B.J. Auerbach, H.J. Harwood Jr., J. R. Kaplan, Old world nonhuman primate models of type 2 diabetes mellitus, ILAR J. 47 (3) (2006) 259–271.
[32] J.E. Fincham, A.J. Benade, M. Kruger, C.M. Smuts, E. Gobregts, D.O. Chalton, D. Kritchevsky, Atherosclerosis: aortic lipid changes induced by diets suggest diffuse disease with focal severity in primates that model human atheromas, Nutrition 14 (1) (1998) 17–22.
[33] K. Kavanagh, K.L. Jones, J. Sawyer, K. Kelley, J.J. Carr, J.D. Wagner, L.L. Rudel, Trans fat diet induces abdominal obesity and changes in insulin sensitivity in monkeys, Obesity 15 (7) (2007) 1675–1684.
[34] D. Pesta, E. Gnaiger, High-resolution respirometry: OXPHOS protocols for human cells and permeabilized fibers from small biopsies of human muscle, Methods Mol. Biol. 810 (2012) 25–58.
[35] M. Picard, T. Taivassalo, D. Ritchie, K.J. Wright, M.M. Thomas, C. Romestaing, R. T. Hepple, Mitochondrial structure and function are disrupted by standard isolation methods, PLoS One 6 (3) (2011) e18317.
[36] M.S. Bharadwaj, D.J. Tyrrell, M.F. Lyles, J.L. Demons, G.W. Rogers, A.J. Molina, Preparation and respirometric assessment of mitochondria isolated from skeletal muscle tissue obtained by percutaneous needle biopsy, J. Vis. Exp. 96 (2015).
[37] B.K. Chacko, D. Zhi, V.M. Darley-Usmar, T. Mitchell, The bioenergetic health index is a sensitive measure of oxidative stress in human monocytes, Redox Biol. 8 (2016) 43–50.
[38] K.H. Kim, Y.T. Jeong, H. Oh, S.H. Kim, J.M. Cho, Y.N. Kim, S.S. Kim, D.H. Kim, K. Y. Hur, H.K. Kim, T. Ko, J. Han, H.L. Kim, J. Kim, S.H. Back, M. Komatsu, H. Chen, D.C. Chan, M. Konishi, N. Itoh, C.S. Choi, M.S. Lee, Autophagy deficiency leads to protection from obesity and insulin resistance by inducing Fgf21 as a mitokine, Nat. Med. 19 (1) (2013) 83–92.
[39] T.C. Register, M.J. Jayo, C.P. Jerome, Oral contraceptive treatment inhibits the normal acquisition of bone mineral in skeletally immature young adult female monkeys, Osteoporos. Int. 7 (4) (1997) 348–353.
[40] E. Bonora, G. Targher, M. Alberiche, R.C. Bonadonna, F. Saggiani, M.B. Zenere, T. Monauni, M. Muggeo, Homeostasis model assessment closely mirrors the glucose clamp technique in the assessment of insulin sensitivity: studies in subjects with various degrees of glucose tolerance and insulin sensitivity, Diabetes Care 23 (1) (2000) 57–63.
[41] B.K. Chacko, P.A. Kramer, S. Ravi, M.S. Johnson, R.W. Hardy, S.W. Ballinger, V. M. Darley-Usmar, Methods for defining distinct bioenergetic profiles in platelets, lymphocytes, monocytes, and neutrophils, and the oxidative burst from human blood, Lab. Investig. 93 (6) (2013) 690–700.
[42] B.P. Dranka, A. Benavides GA FAU - Diers, S. Diers AR FAU - Giordano, B. Giordano S FAU - Zelickson, C. Zelickson BR FAU - Reily, C.F. Reily, L.F. Zou, B. Chatham JC FAU - Hill, J. Hill BG FAU - Zhang, J.F. Zhang, A.F. Landar, V. M. Darley-Usmar, Assessing bioenergetic function in response to oxidative stress by metabolic profiling, J. Biol. Chem. 279 (31) (2004).
[43] C. Desler, T.L. Hansen, J.B. Frederiksen, M.L. Marcker, K.K. Singh, R.L. Juel, Is there a link between mitochondrial reserve respiratory capacity and aging? J. Aging Res. 2012 (2012) 192503.
[44] D.A. Ferrick, A. Neilson, C. Beeson, Advances in measuring cellular bioenergetics using extracellular flux, Drug Discov. Today 13 (5–6) (2008) 268–274.
[45] M.B. Jekabsons, D.G. Nicholls, In situ respiration and bioenergetic status of mitochondria in primary cerebellar granule neuronal cultures exposed continuously to glutamate, Free Radic. Biol. Med. 51 (9) (2011).
[46] C.G. Perry, D.A. Kane, C.T. Lin, R. Kozy, B.L. Cathey, D.S. Lark, C.L. Kane, P. M. Brophy, T.P. Gavin, E.J. Anderson, P.D. Neufer, Inhibiting myosin-ATPase reveals a dynamic range of mitochondrial respiratory control in skeletal muscle, Biochem. J. 437 (2) (2011) 215–222.
[47] M.S. Bharadwaj, D.J. Tyrrell, I. Leng, J.L. Demons, M.F. Lyles, J.J. Carr, B.J. Nicklas, A.J. Molina, Relationships between mitochondrial content and bioenergetics with obesity, body composition and fat distribution in healthy older adults, BMC Obes. 2 (2015) 40.
[48] G.W. Rogers, M.D. Brand, S. Petrosyan, D. Ashok, A.A. Elorza, D.A. Ferrick, A. N. Murphy, High throughput microplate respiratory measurements using minimal quantities of isolated mitochondria, PLoS One 6 (7) (2011) e21746.
[49] S. Furukawa, T. Fujita, M. Shimabukuro, M. Iwaki, Y. Yamada, Y. Nakajima, O. Nakayama, M. Makishima, M. Matsuda, I. Shimomura, Increased oxidative stress in obesity and its impact on metabolic syndrome, J. Clin. Investig. 114 (12) (2004) 1752–1761.
[50] L.M. Griffiths, N.A. Doudican, G.S. Shadel, P.W. Doetsch, Mitochondrial DNA oxidative damage and mutagenesis in *Saccharomyces cerevisiae*, Methods Mol. Biol. 554 (2009) 267–286.
[51] G.J. Tranah, K. Yaffe, S.M. Katzman, E.T. Lam, L. Pawlikowska, P.Y. Kwok, N. J. Schork, T.M. Manini, S. Kritchevsky, F. Thomas, A.B. Newman, T.B. Harris, A. L. Coleman, M.B. Gorin, E.P. Helzner, M.C. Rowbotham, W.S. Browner, S. R. Cummings, Mitochondrial DNA Heteroplasmy Associations with neurosensory and mobility function in elderly adults, J. Gerontol. A Biol. Sci. Med. Sci. 70 (11) (2015) 1418–1424.
[52] B. CHANCE, G.R. WILLIAMS, A simple and rapid assay of oxidative phosphorylation, Nature 175 (4469) (1955) 1120–1121.
[53] A.M. Joseph, P.J. Adhihetty, T.W. Buford, S.E. Wohlgemuth, H.A. Lees, L.

M. Nguyen, J.M. Aranda, B.D. Sandesara, M. Pahor, T.M. Manini, E. Marzetti, C. Leeuwenburgh, The impact of aging on mitochondrial function and biogenesis pathways in skeletal muscle of sedentary high- and low-functioning elderly individuals, Aging Cell 11 (5) (2012) 801–809.

[54] F. Ambrosio, E. Brown, D. Stolz, R. Ferrari, B. Goodpaster, B. Deasy, G. Distefano, A. Roperti, A. Cheikhi, Y. Garciafigueroa, A. Barchowsky, Arsenic induces sustained impairment of skeletal muscle and muscle progenitor cell ultrastructure and bioenergetics, Free Radic. Biol. Med. (2014).

[55] S. Larsen, J.H. Danielsen, S.D. Sondergard, D. Sogaard, A. Vigelsoe, R. Dybboe, S. Skaaby, F. Dela, J.W. Helge, The effect of high-intensity training on mitochondrial fat oxidation in skeletal muscle and subcutaneous adipose tissue, Scand. J. Med. Sci. Sports (2014).

[56] P.A. Kramer, S. Ravi, B. Chacko, M.S. Johnson, V.M. Darley-Usmar, A review of the mitochondrial and glycolytic metabolism in human platelets and leukocytes: implications for their use as bioenergetic biomarkers, Redox Biol. 2 (2014) 206–210.

[57] M.D. Brand, D.G. Nicholls, Assessing mitochondrial dysfunction in cells, Biochem. J. 435 (2) (2011) 297–312.

[58] N. Cardenes, C.F. Corey, L.F. Geary, S. Jain S FAU - Zharikov, S. Zharikov S FAU - Barge, E. Barge S FAU - Novelli, S. Novelli EM FAU - Shiva, S. Shiva, Platelet bioenergetic screen in sickle cell patients reveals mitochondrial complex V inhibition, which contributes to platelet activation, Blood 123 (2014) 2864–2872 (1528-0020 (Electronic)).

[59] N. Stride, M. Larsen S FAU - Hey-Mogensen, M.F. Hey-Mogensen, C. Hansen CN FAU - Prats, C.F. Prats, D.F. Steinbruchel, L.F. Kober, F. Dela, Impaired mitochondrial function in chronically ischemic human heart, Am. J. Physiol. Heart Circ. Physiol. (2013) 1407–1414 (1522-1539 (Electronic)).

[60] R.A. Jacobs, C.F. Siebenmann, M.F. Hug, M.F. Toigo, C. Meinild AK FAU - Lundby, C. Lundby, Twenty-eight days at 3454-m altitude diminishes respiratory capacity but enhances efficiency in human skeletal muscle mitochondria, FASEB J. (2012) 5192–5200 (1530-6860 (Electronic)).

[61] S.Y. Park, J.R. Gifford, R.H. Andtbacka, J.D. Trinity, J.R. Hyngstrom, R.S. Garten, N.A. Diakos, S.J. Ives, F. Dela, S. Larsen, S. Drakos, R.S. Richardson, Cardiac, skeletal, and smooth muscle mitochondrial respiration: are all mitochondria created equal? Am. J. Physiol. Heart Circ. Physiol. (2014) 346–352 (1522–1539 (Electron.)).

[62] J.K. Salabei, A.A. Gibb, B.G. Hill, Comprehensive measurement of respiratory activity in permeabilized cells using extracellular flux analysis, Nat. Protoc. 9 (2) (2014) 421–438.

[63] P.A. Kramer, B.K. Chacko, D.J. George, D. Zhi, C.C. Wei, L.J. Dell'Italia, S.J. Melby, J.F. George, V.M. Darley-Usmar, Decreased Bioenergetic Health Index in monocytes isolated from the pericardial fluid and blood of post-operative cardiac surgery patients, Biosci. Rep. 35 (4) (2015).

[64] A.CzajkaS.AjazL.GnudiC.K.ParsadeP.JonesF.ReidA.N.Malik, Altered Mitochondrial Function, Mitochondrial DNA and Reduced Metabolic Flexibility in Patients with Diabetic Nephropathy. (2352–3964 (Electronic)).

[65] Q. Zhang, M. Raoof, Y. Chen, Y. Sumi, T. Sursal, W. Junger, K. Brohi, K. Itagaki, C. J. Hauser, Circulating mitochondrial DAMPs cause inflammatory responses to injury, Nature 464 (7285) (2010) 104–107.